# Fatigue Behaviour of Concrete in Tension

C.Kessler-Kramer, V.Mechtcherine & H.S.Müller
*Institute of Concrete Structures and Building Materials, Karlsruhe, Germany*

ABSTRACT: Deformation controlled uniaxial tensile tests on dog-bone shaped prisms as well as on notched prisms were carried out to determine the fatigue behaviour of concrete. The test results show a significant increase of the uniaxial tensile strength, the Young's Modulus and the elongation at failure with increasing the strain rate. The net tensile strength, the fracture energy, the characteristic length as well as the deformation at the peak stress decrease for an increasing number of load cycles. Further, the envelope curves of the stress-deformation relation obtained from the high-cycle fatigue tests differ significantly from the corresponding curve from the tests with a monotonic loading. On the basis of the experimental results, a new rheological statistical model considering in particular the number of load cycles, time effects and the heterogeneity of concrete was developed.

## 1 INTRODUCTION

For safety and economical reasons a profound knowledge of the fatigue behaviour of concrete and concrete structures as well as corresponding constitutive laws are required. However, the existing constitutive relations are based on experimental investigations with a low number of load cycles which are generally of minor interest for practical design.

The fatigue experiments with a higher number of load cycles have always been stress controlled Wöhler tests until now. Such tests do not allow to study the softening behaviour of concrete after reaching the peak load.

Preliminary to this study an extensive literature survey was carried out to identify the relevant parameters influencing the fatigue behaviour of concrete under monotonic and cyclic tensile loads. It could be shown that several parameters, e.g. the compressive strength, the maximum aggregate size or the content of cement may be neglected if the mechanical and the fracture mechanical properties obtained in fatigue experiments are related to the corresponding material parameters received under static loading conditions. For some other parameters, e.g. the strain rate or a preloading, no consistent conclusion could be drawn by comparing the findings of different authors. The effect of the number of load cycles to failure has not been investigated at all.

Therefore, in this investigation the fracture processes in concrete under low-cycle and high-cycle fatigue loading were studied in order to describe the fatigue behaviour of concrete on the basis of fracture mechanical conceptions.

## 2 EXPERIMENTAL PROGRAMME

### 2.1 *Geometry of the investigated specimens*

In the experimental part of the study a series of deformation controlled uniaxial tension tests on dog-bone shaped as well as on notched concrete prisms were carried out. Figure 1 shows a schematic view of the geometry of the two types of specimens used in the experimental programme.

The dog-bone shaped prisms were used to study the pre-peak behaviour of the stress-strain relations in order to receive reliable values of the uniaxial ten-
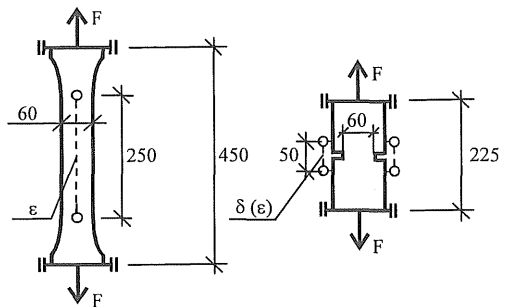


Figure 1. Geometrical dimensions of the investigated specimens (thickness of both specimens d = 100; data in [mm]).

sile strength $f_t$, the Young's Modulus (tangent modulus of elasticity) $E_0$ and the elongation at failure (peak stress) $\varepsilon_{tu}$ to be included in a subsequent numerical calculation. On the notched prisms monotonic as well as low-cycle and high-cycle fatigue tension tests were carried out to obtain the softening behaviour of concrete under such loading conditions.

Besides the geometrical dimensions of the concrete specimens the gauge lengths of 250 mm for the dog-bone shaped prisms and 50 mm for the notched prisms are indicated in Figure 1.

## 2.2 Concrete composition and preparation of the specimens

The composition of the investigated concrete is given in Table 1. For the mixture ordinary Portland cement CEM I 32.5 R was used. As aggregate quartzite Rhine sand and gravel with a maximum aggregate size of 16 mm were applied.

Table 1. Composition of the concrete.

| Water-cement ratio | | 0.55 | |
|---|---|---|---|
| Cement | CEM I 32.5 R | 318 | kg/m³ |
| Aggregate | 0/2 mm | 555 | kg/m³ |
| | 2/8 mm | 703 | kg/m³ |
| | 8/16 mm | 592 | kg/m³ |
| Superplasticizer | | 1.20 | kg/m³ |

All specimens were cast horizontally in metal forms. After demoulding at an age of one day, an aluminium foil was glued by means of an epoxy resin to the specimens termed as sealed. Additionally a thin polyethylene foil was wrapped around the specimens to complete the protection against desiccation. Furthermore, the zone where the crack was expected was wrapped directly with polyethylene foil in order to avoid a contribution of the epoxy resin to the bearing capacity of the concrete specimens. Continuous control of the weight should proof the quality of the chosen sealing. With this kind of curing the moisture condition of mass concrete should be simulated.

The specimens termed as unsealed were stored in a climatic chamber with a relative humidity of 65 % and a temperature of 20 °C immediately after demoulding. These specimens represent the moisture condition of slender concrete members without proper curing.

## 2.3 Characteristics of the used concrete

The properties of fresh and hardened concrete are given in Table 2. The compressive strength as well as the Young's Modulus were obtained at a concrete age of 28 days. The values for the standard deviation are given in parentheses.

Table 2. Properties of the investigated concrete.

| Slump | 39.0 (3.7) | cm |
|---|---|---|
| Air void contents | 1.20 (0.19) | Vol.-% |
| Gross density | 2407 (9) | kg/m³ |
| Compressive strength obtained on cube specimens | 48.0 (2.1) | MPa |
| Young's Modulus | 27750 (1270) | MPa |

## 2.4 Loading regime

Since a very stiff test set-up is required for the deformation controlled cyclic tests all tests have been performed with non-rotatable boundary conditions. Therefore, the concrete specimens have been glued with an extra strong two component glue to stiff metal adapters, which were firmly connected to the bearing platens of the testing machine.

The mean value of two LVDTs measuring strains for a basis length of 250 mm on the dog-bone shaped prisms and 50 mm on the notched prisms was used as control signal for the testing machine to run the tests with the desired deformation rate (compare Fig. 1).

The basic approach for the test control in the fatigue experiments is shown in Figure 2. The increase of the total deformation within the gauge length corresponding to the crack opening is given by the deformation increment $\Delta\delta$ which was kept constant from cycle to cycle, i.e. $\Delta\delta = d\delta/dn = const.$, where n = number of load cycles. When the preset value for the deformation $\Delta\delta$ in the following cycle is reached the specimen will be unloaded until the lower reversal point is attained.

The lower reversal point $\delta_{min}$ was defined as a function of the lower load level $F_{min} = 0$ for all experiments. A definition of the lower reversal point $\delta_{min}$ by means of the deformation is unsuitable, since unlocked or pulled out aggregates or hardened cement paste particles may dislocate while the crack is
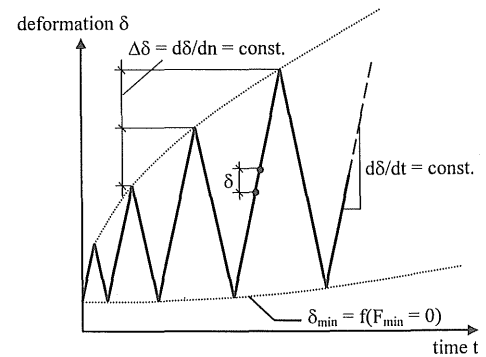


Figure 2. Test control in the fatigue experiments.

open and lead to local tensile as well as compressive stresses in the case of unloading. This effect results in a progressive crack opening without any loading at the time of measuring the deformation.

Also the deformation rate $d\delta/dt$ was kept constant throughout the complete loading cycle.

The deformation increment $\Delta\delta$ was determined by dividing the critical crack opening (i.e. the crack opening at which no tensile stresses can be transmitted any more across the crack) defined from the monotonic tests by the desired number of load cycles to failure. As maximum crack opening in the monotonic case a constant value of $w_{cr} = 160$ μm was chosen from the literature, see Hordijk (1991). Taking an average value from the own experimental results was not possible since the monotonic and the cyclic tests were done at the same time in order to eliminate possible effects of using different concrete mixes.

## 2.5 *Test parameters*

The main parameters in the experiments were the number of cycles to failure ranging from monotonic loading to 100,000 load cycles and the curing conditions, see paragraph 2.2.

The tests were performed on normal strength concrete applying two different strain rates. For the tests on the dog-bone shaped prisms $\dot\varepsilon_1 = 10^{-4}$ 1/s and $\dot\varepsilon_2 = 10^{-5}$ 1/s were chosen. The experiments on the notched prisms were performed with $\dot\delta_1 = 5$ μm/s and $\dot\delta_2 = 0.5$ μm/s corresponding to the above mentioned strain rates with the gauge length of 50 mm.

Other interesting parameters such as the lower stress level, the age of concrete at testing etc. were kept constant within the experimental programme.

The age of the concrete at testing was 280 days. For each investigated parameter combination at least five specimens were tested.

# 3 EXPERIMENTAL RESULTS

## 3.1 *Tests on dog-bone shaped prisms*

The main results of the uniaxial tension tests on the dog-bone shaped prisms are given in Table 3. Hereby, the standard deviation is given in parentheses.

For a better illustration the results are shown in Figure 3. The effect of the strain rate on the uniaxial tensile strength $f_t$ (left), on the Young's Modulus $E_0$ (middle) and on the elongation at failure $\varepsilon_{tu}$ (right) is shown for the sealed as well as for the unsealed specimens. It can be concluded that an increase of the strain rate by a factor 10 leads to higher values of all three investigated parameters. This corresponds well with the findings by Reinhardt et al. (1990) or Mechtcherine et al. (1995). Further, the sealed

specimens provided always higher values than the unsealed specimens.

Table 3. Results of the tests on the dog-bone shaped prisms.

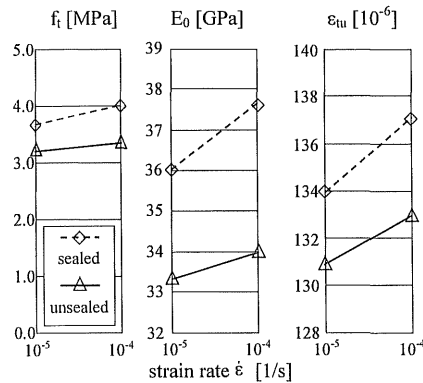|  | sealed | unsealed |
| --- | --- | --- |
| Uniaxial tensile strength $f_t$ [MPa] | | |
| $\dot\varepsilon_1 = 10^{-4}$ 1/s: | 4,01 (0,28) | 3,35 (0,13) |
| $\dot\varepsilon_2 = 10^{-5}$ 1/s: | 3,68 (0,27) | 3,21 (0,13) |
| Young's Modulus $E_0$ [MPa] | | |
| $\dot\varepsilon_1 = 10^{-4}$ 1/s: | 37649 (1922) | 33926 (2003) |
| $\dot\varepsilon_2 = 10^{-5}$ 1/s: | 36010 (1382) | 33435 (1732) |
| Elongation at failure $\varepsilon_{tu}$ [$10^{-6}$] | | |
| $\dot\varepsilon_1 = 10^{-4}$ 1/s: | 137 (13) | 133 (6) |
| $\dot\varepsilon_2 = 10^{-5}$ 1/s: | 134 (8) | 131 (7) |



Figure 3. Effect of the strain rate and the curing conditions on the uniaxial tensile strength (left), the Young's Modulus (middle) and the elongation at failure (right).

As can be seen by the different gradients of the lines in Figure 3 the effect of increasing the strain rate is more pronounced for the sealed specimens.

## 3.2 *Tests on notched concrete specimens*

The experimental results obtained from the tests on the notched concrete prisms show that with an increasing number of load cycles the maximum load and therefore the net tensile strength $f_{tn}$ decreases (Fig. 4). In the low-cycle region up to 100 load cycles the $f_{tn}$-values remain approximately constant for the sealed specimens or increase slightly for the unsealed specimens. This observation is in accordance with the experimental findings on three-point bend tests on notched concrete beams, see Kessler & Müller (1998).

Further, an increase of the number of load cycles leads to an increase of the critical crack opening where the transferable tensile stress approaches zero,

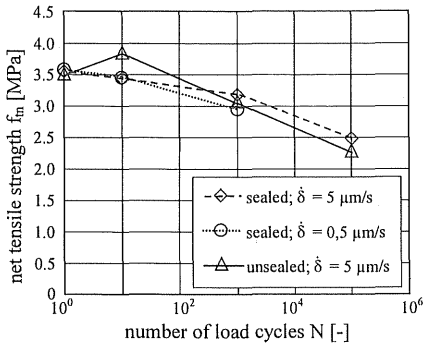whereas a decrease of the deformation at the peak stress $\delta_{tu}$ could be observed (Fig. 5).



Figure 4. Effect of the number of load cycles to failure on the net tensile strength for different deformation rates and curing conditions.
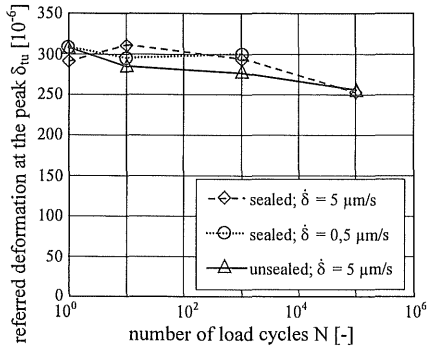


Figure 5. Effect of the number of load cycles to failure on the deformation at the peak stress for different deformation rates and curing conditions.

For both mechanical properties – the net tensile strength $f_{tn}$ and the deformation at the peak stress $\delta_{tu}$ – the values for the unsealed specimens are mostly lower than the corresponding values for the sealed specimens. This agrees with the results obtained from the tests on the dog-bone shaped prisms. Compared with the tests on the dog-bone shaped prisms the effect of the strain rate in the experiments on notched concrete prisms is less pronounced.

Figure 6 shows that in the high-cycle tests the fracture energy $G_F$ decreases as the number of load cycles increases. The $G_F$-values were calculated as the area under the measured stress-deformation curves. In the case of cyclic tests the envelope curves of the corresponding stress-deformation relations have been chosen. Therefore, a possible contribution of the area within the hysteresis loops was not considered.

At this point it is worth to mention that an experimental determination of $G_F$-values by means of
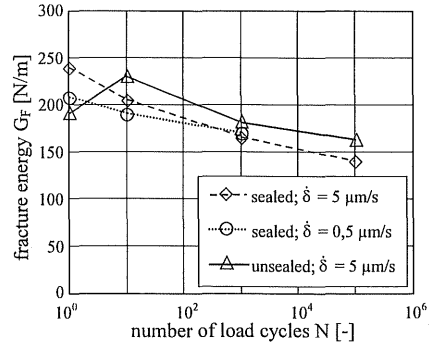


Figure 6. Effect of the number of load cycles to failure on the fracture energy for different deformation rates and curing conditions.

three-point bend tests without dead weight compensation in a foregoing investigation (see Kessler & Müller 1998) could not show this clear dependency of the fracture energy on the number of load cycles to failure. This results from the fact that an estimation of the contribution of the energy due to the dead weight turned out to be about 50 % of the total energy.

Additionally, the characteristic length $l_{ch}$ of the prisms has been investigated. The characteristic length $l_{ch}$ is a fracture mechanical parameter characterizing the brittleness of a material. Lower $l_{ch}$-values indicate a higher brittleness. It can be calculated using Equation 1:

$$l_{ch} = \frac{G_F \cdot E_0}{f_t^2} \qquad (1)$$

The values for $f_t$ and $E_0$ were taken from the corresponding tests on the dog-bone shaped prisms.

Figure 7 clearly shows that with an increasing number of load cycles the characteristic length decreases indicating a more brittle behaviour of the concrete. The $l_{ch}$-values for the unsealed specimens
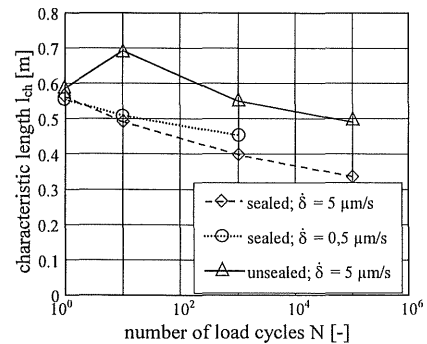


Figure 7. Effect of the number of load cycles to failure on the characteristic length for different deformation rates and curing conditions.

were always above the corresponding values for the sealed specimens.

# 4 DISCUSSION

## 4.1 Effect of the strain rate

The reason for the higher $f_t$-values with an increasing strain rate can be found considering the crack development in concrete as a function of time. The cracks always strike the path with the lowest resistance, which runs along the aggregates for normal strength concrete. If the rate of loading is higher the cracks can grow faster because of the faster energy supply. Therefore, some of the cracks go straight through the aggregates following the shortest distance to cover.

## 4.2 Effect of the curing conditions

The higher $f_t$-values for the sealed specimens compared to the unsealed specimens may be due to the fact that the hydration of the sealed specimens could reach a higher degree in the whole concrete prism whereas the unsealed specimens were allowed to desiccate at the surfaces. The desiccation leads not only to a lower degree of the hydration but also to pronounced moisture gradients throughout the cross section which finally results in bond cracks between the aggregates and the matrix. These bond cracks are already formed mainly due to shrinkage effects.

This phenomenon is even more pronounced by the so called wall effect resulting from the kind of making the specimens in individual moulds. This leads to higher contents of cement matrix near the moulded surfaces resulting in a more brittle and fragile concrete quality than in the middle of the specimens. The higher content of cement matrix leads to a higher number of microcracks due to shrinkage.

The reason for the fact that the effect of increasing the strain rate is more emphasized for the sealed specimens may result from the so called Stéfan effect, see e.g. Rossi & Toutlemonde (1996). The Stéfan effect delays the creation of the microcracks before the localization of the failure and tends to counter the propagation of the macrocracks after the localization.

The reason for the higher $l_{ch}$-values for the unsealed specimens compared to the values obtained on the sealed specimens could be a more distinctive aggregate interlocking across small microcracks, see Mechtcherine & Müller (2001).

## 4.3 Effect of the number of load cycles

The main finding in the study is that for an increasing number of load cycles the envelope curves of the $\sigma$-$\delta$-relations differ significantly from the corresponding monotonic curve, see Figure 8. The ascending branches show approximately the same shape and the same stiffness for all curves. Because of the lower $f_{tn}$-values for the high-cycle fatigue tests (Fig. 4) these curves are below the curves for the monotonic and the low-cycle fatigue tests in the first, steeper part of the stress-deformation relation. This also leads to the lower $G_F$-values (Fig. 6) with an increasing number of load cycles which is mainly due to a lower energy consumption in this part of the softening curve. Additionally, the curves from the high-cycle fatigue tests are steeper than the curves for the monotonic and the low-cycle fatigue tests, see Figure 8.

In the second, shallow part of the softening curve the average curve for the cyclic tests with 1000 load cycles intersects the average curve with 10 load cycles. Nevertheless, the contribution of the second part of the softening curve to the value of the fracture energy is limited, since it covers a minor amount of energy compared to the first part of the softening curve. This intersection could not be observed for the monotonic nor the $\sigma$-$\delta$-relation for 100,000 load cycles.
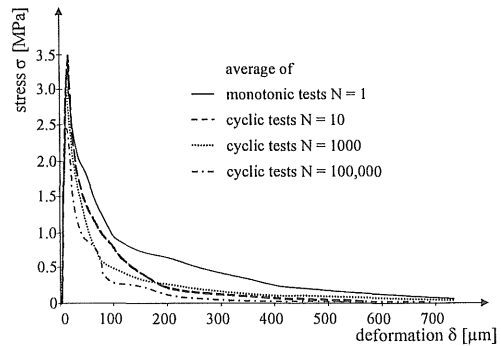
Figure 8. Envelope curves of the stress-deformation relations obtained from the monotonic and the fatigue tests performed on sealed specimens.

The mentioned observations clearly show that the conventional assumption of an unique envelope curve for the fatigue behaviour of concrete cannot be maintained especially for high-cycle fatigue loading.

## 4.4 Modelling the behaviour of concrete under tensile fatigue loading

The obtained experimental results restricts the validity of the existing constitutive relations to the range of low-cycle fatigue since they are completely based on the fore-mentioned assumption, see e.g. Duda (1991) or Hordijk (1991).

Based on these results, a new constitutive law on the basis of a rheological statistical model considering in particular the number of load cycles, time ef-

fects and the heterogeneity of concrete is currently developed (Fig. 9). The model consists of simple rheological elements like springs, friction blocks and dashpots representing the elastic, frictional and viscous deformation components of concrete. The hysteresis loops are described by a serial arrangement of two friction blocks and two spring elements. This combination follows an idea originally introduced by Duda (1991). Additionally, a serially arranged dashpot considers the rate dependency of concrete and enables to include effects like e.g. the load history. A parallel arrangement of a friction block allows for the effect that unlocked or pulled out aggregates or hardened cement paste particles may dislocate while the crack is open and lead to local tensile as well as compressive stresses in the case of unloading.
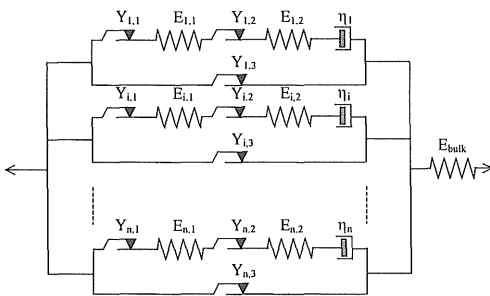


Figure 9. Rheological statistical model for the description of the fatigue behaviour of concrete under tensile loading conditions.

The combination of these rheological elements is statistically distributed following an exponential function after Weibull to reflect the heterogeneity of concrete. The bulk behaviour of the undamaged concrete is considered by an additional spring element.

This rheological statistical model forms the basis of a constitutive law for the description of the stress-crack opening relation of concrete under tensile fatigue loading.

5 SUMMARY AND CONCLUSIONS

In this study the effects of the number of load cycles to failure, the strain rate and the curing conditions on mechanical and fracture mechanical parameters of concrete under monotonic and cyclic tensile loading were investigated. Therefore, deformation controlled uniaxial tensile tests on dog-bone shaped prisms as well as on notched prisms have been carried out.

The tests on dog-bone shaped prisms showed a significant increase of the uniaxial tensile strength $f_t$, the Young's Modulus $E_0$ and the elongation at fail-

ure $\varepsilon_{tu}$ with an increase of the strain rate by a factor 10. For the sealed specimens the values of these three parameters were found to be higher than for the unsealed ones. Further, the increase of the $f_t$-, $E_0$- and $\varepsilon_{tu}$-values was more pronounced in the case of the sealed specimens.

Concerning the tests on notched concrete prisms the net tensile strength $f_{tn}$ as well as the deformation at the peak stress $\delta_{tu}$ decreases with an increasing number of load cycles. The fracture energy $G_F$ and the characteristic length $l_{ch}$ decrease with an increasing number of load cycles as well. Hereby, the $G_F$- and $l_{ch}$-values are higher for the tests on unsealed specimens.

It could be shown that for an increasing number of load cycles the corresponding envelope curves of the stress-deformation relation differ significantly from the monotonic curve. This observation also restricts the validity of all existing material laws to the low-cycle region. A new constitutive law based on a rheological statistical model is currently developed.

REFERENCES

Duda, H. 1991. *Bruchmechanisches Verhalten von Beton unter monotoner und zyklischer Zugbeanspruchung.* Schriftenreihe des Deutschen Ausschusses für Stahlbeton, Heft 419.
Hordijk, D.A. 1991. *Local Approach to Fatigue of Concrete.* Dissertation. Delft University of Technology, Delft.
Kessler, C. & Müller, H.S. 1998. Experimental Investigations on Fracture and Damage of Concrete due to Fatigue. In H. Mihashi & K. Rokugo (ed.), *Fracture Mechanics of Concrete Structures; Proc. FRAMCOS-3, Gifu, October 12-16 1998.* Freiburg: Aedificatio.
Mechtcherine, V., Garrecht, H. & Hilsdorf, H.K. 1995. Effect of Temperature and Loading Rate on Fracture Mechanical Behaviour of Concrete Subjected to Uniaxial Tension. In F. Wittmann (ed.), *Fracture Mechanics of Concrete Structures; Proc. FRAMCOS-2, Zurich, July 25-28 1995.* Freiburg: Aedificatio.
Mechtcherine, V. & Müller, H.S. 2001. Fractological Investigations on the Fracture in Concrete. In R. de Borst (ed.), *Fracture Mechanics of Concrete Structures; Proc. FRAMCOS-4, Cachan, May 28 – June 2 2001.* Rotterdam: Balkema.
Reinhardt, H.W., Rossi, P. & Van Mier, J.M.G. 1990. Joint Investigation of Concrete at High Rates of Loading. *Materials and Structures* (23): 213-216.
Rossi, P. & Toutlemonde, F. 1996. Effect of the Loading Rate on the Tensile Behaviour of Concrete: Description of the Physical Mechanisms. *Materials and Structures* (29): 116-118.